ELSEVIER

Contents lists available at ScienceDirect

Extreme Mechanics Letters

journal homepage: www.elsevier.com/locate/eml



Stress-corrosion cracking of polypropylene in harsh oxidizing environments



Jong-hyoung Kim ^{a,1}, Won-Seok Song ^{a,b,1}, Quan Jiao ^a, Joost J. Vlassak ^{a,*}

- ^a School of Engineering and Applied Sciences, Harvard University, Cambridge MA, USA
- b Infra Technology Center, Global Infra Technology, Samsung Electronics, Gyeonggi-do, South Korea

ARTICLE INFO

Article history:
Received 13 April 2023
Received in revised form 25 July 2023
Accepted 2 September 2023
Available online 11 September 2023

Keywords:
Semiconductor industry
Polyolefin drainage pipes
Oxidizing environment
Dilute Piranha solution
Stress corrosion cracking
Subcritical crack growth

ABSTRACT

Thermoplastic pipes are widely used in the semiconductor industry, where they are used to drain highly corrosive liquid waste. When exposed to oxidizing environments, thermoplastic pipes can undergo stress-corrosion cracking (SCC), potentially causing them to fail prematurely in the absence of appropriate design and maintenance guidelines. Here, the stress-corrosion cracking behavior of polypropylene, commonly used in waste drainage pipes for dilute sulfuric acid/hydrogen peroxide mixtures (Piranha solutions), is investigated as a function of applied energy release rate. Sub-critical crack growth experiments are performed with compact tension specimens in sulfuric acid/hydrogen peroxide mixtures using a custom constant-force loading system to evaluate the effects of temperature and chemical composition on SCC crack growth. The activation energy for the SCC process is $99.7\,\pm\,15.3$ kJ/mol, and the crack growth rate depends sensitively on the concentrations of sulfuric acid and hydrogen peroxide in the mixture. We propose a practical guideline to calculate the service life of polypropylene pipes in Piranha solutions using crack velocity curves and show that accidental exposure to a concentrated Piranha solution can significantly reduce service life.

© 2023 Elsevier Ltd. All rights reserved.

1. Introduction

The size of the semiconductor market has grown tremendously over the last decade, reaching \$580 billion in 2022². This explosive growth has led to a rapid expansion of semiconductor production facilities worldwide. The US administration recently passed legislation, including the Creating Helpful Incentives to Produce Semiconductors (CHIPS) for America Act, to provide \$52 billion in federal investment to promote semiconductor production in the US.³ Since the fabrication of semiconductor devices is carried out with repeated cleaning and etching steps, each fabrication facility requires thousands of kilometers of pipes to transport large amounts of fresh and waste chemicals. Thermoplastic pipes are widely used for this purpose due to their

* Corresponding author. E-mail address: vlassak@seas.harvard.edu (J.J. Vlassak).

low cost and ease of installation. The thermoplastic most commonly used is polypropylene because of its lightweight, excellent chemical resistance, heat resistance, and mechanical properties. Polypropylene is also much less expensive and easier to process than fluoropolymers. Generally, thermoplastic pipes are installed following standards and codes such as DIN-DVS 2205. These standards provide guidelines mainly on creep behavior, but do not consider environmentally assisted fracture in oxidizing environments. When designing transport systems for dilute oxidizing chemicals, stakeholders generally select pipe materials by referring to compatibility charts between plastic materials and chemicals. The compatibility charts found in the literature [1-3], however, have limited information and do not provide clear guidelines on how to use these materials for diluting chemicals under broad conditions. When these materials are used in the wrong environment in the presence of residual stresses, stresscorrosion cracking (SCC) can lead to fractures or leaks before the end of the expected service life (Fig. 1a). This phenomenon of stress-corrosion cracking was first observed in polyethylene in various chemical environments in the 1950s [4].

During chemical degradation in oxidizing environments, the molecular weight of thermoplastics generally decreases due to chain scission and micro-cracks form on the surface of the polymer [5]. When tension is applied to thermoplastics in oxidizing environments, these cracks can grow rapidly, even at stresses well below the elastic limit (Fig. 1b). The crack tip generally

¹ Jong-hyoung Kim and Won-Seok Song contributed equally to this work.

WSTS, SIA. (2022). Semiconductor market size worldwide from 1987 to 2023 (in billion U.S. dollars). Statista. Statista Inc. Accessed: February 14, 2023. https://www.statista.com/statistics/266973/global-semiconductorsales-since-1988/

³ The White House. (2022). Fact sheet: Biden-Harris Administration bringing Semiconductor Manufacturing Back to America. Accessed: June 8, 2022. https://www.whitehouse.gov/briefing-room/statements-releases/2022/01/21/fact-sheet-biden-harris-administration-bringing-semiconductor-manufacturing-back-to-america-2/

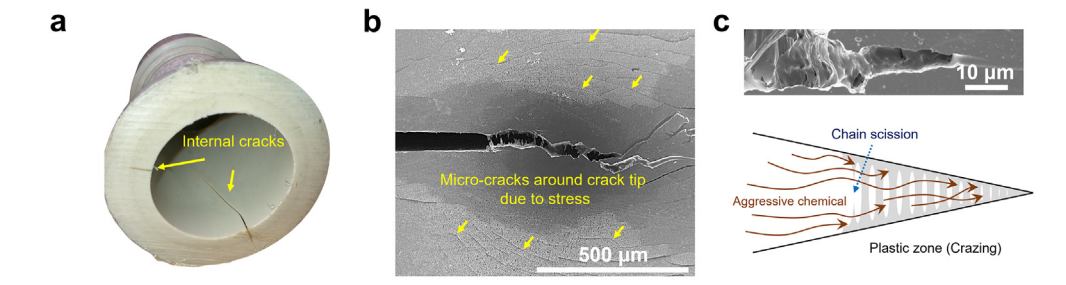


Fig. 1. (a) Failed polypropylene component due to SCC; (b) SEM image of polypropylene suffering from SCC in a Piranha solution; (c) SEM image of the crack tip and molecular processes of stress corrosion cracking near a crack tip in polyolefin.

has the shape shown in Fig. 1c. Oxidizing species diffuse to the deformed crack tip, where they react with the stretched fibrils in the crack process zone resulting in chain scission (Fig. 1c). Several theoretical studies have been performed to understand the mechanisms responsible for stress-corrosion cracking and analytical models have been proposed [5–8]. These models provide a detailed description of SCC in thermoplastics but are challenging to use in practice because they require many parameters for each case. Quantitative experimental measurements of crack growth rates in oxidizing environments are not readily available. Thus, there is a need for sub-critical crack growth experiments to characterize the propagation of cracks in thermoplastics in various environments such as have been performed for many other types of materials [9–12].

Here, we study the SCC of polypropylene in a harsh oxidizing aqueous environment relevant to semiconductor production using sub-critical crack growth testing. In particular, we evaluate the SCC of polypropylene in the Piranha solution, a mixture of concentrated sulfuric acid and hydrogen peroxide that forms peroxymonosulfuric acid, also known as Caro's acid, one of the strongest known oxidizers. We investigate the effects of temperature and concentration of the Piranha solution on the crack growth rate as a function of the energy release rate. Based on the results of this study, we propose practical guidelines for the safe use of polypropylene or other thermoplastics in strongly oxidizing environments.

2. Materials and methods

We prepared our test specimens using commercial polypropylene homopolymer (Borealis Beta-PPH) with a density of 0.91 g/cm³ and a melt flow index of 0.5 g/10 min. The crystallinity was 50% as determined by differential scanning calorimetry (DSC) (Appendix A). Young's modulus was measured to be 1216 \pm 32 MPa at room temperature (19 °C) according to ASTM D638. The polypropylene was supplied in plates with thicknesses of 2.0 and 20 mm

The Piranha solution was prepared as a 3:1 mixture of 93% sulfuric acid and 30% hydrogen peroxide. Since the preparation of Piranha solution involves a very exothermic reaction with a significant risk of explosion if mixed too quickly, the hydrogen peroxide was added dropwise to the sulfuric acid. Appropriate personal protective equipment was worn at all times while preparing or handling Piranha solutions [13].

Sub-critical crack growth experiments were performed with compact tension (CT) specimens using a customized constant-force loading system (Fig. 2a and 2b) to avoid any issues related to time-dependent deformation of polypropylene [14]. No significant deformation was observed when specimens were loaded in air for extended periods of time (up to nine days at room

temperature) under typical test conditions, implying that the applied energy release rate was not affected by creep. For safety, (1) we installed the testing part of the setup including the fixtures and the container with the Piranha solution inside a fume hood, (2) we used a multi-pulley system to apply a large constant force to the specimen using a relatively small dead weight, and (3) to prevent spilling of the Piranha solution on sample failure. we limited the maximum displacement of the sample fixture by installing a safety lock on the test specimen and by placing a block underneath the dead weight to limit its travel. The multipulley system amplified the force exerted by the weight by a factor of 8.94. This amplification factor was close to the ideal value of 9.0 due to the use of low-friction blocks. Compact tension specimens with a thickness B of 20 mm and width W of 40 mm were prepared according to the ASTM D5045 standard. The initial notches were prepared by machining and then sharpened using a razor blade.

To determine the crack velocity in the sub-critical crack growth experiments, the crack length was measured as a function of time using a digital camera. During the experiments, the specimen was submerged in the Piranha solution. To measure the crack length, a vertical translation stage was used to lower the container with the Piranha solution and expose the sample, thus avoiding any measurement errors due to bubbles on the specimen surface. Experiments were performed at 30 °C, 40 °C, 50 °C, and 60 °C with a 100% Piranha solution. During these tests, the Piranha solution was replaced daily to prevent loss of reactivity. To evaluate the effect of concentration, experiments were also performed in solutions in which the Piranha solution was diluted to 90%, 85%, and 75% of the nominal solution by adding deionized water as appropriate. These measurements were performed at 50 °C.

The energy release rate was calculated for each measured crack length *a* using Eq. (1) following ASTM D5045:

$$G = \frac{(1 - v^2)F^2}{E \cdot W \cdot B^2} f(x), \tag{1}$$

where x = a/W, and $f(x) = \frac{(2+x)^2(0.886+4.64x-13.32x^2+14.72x^3-5.6x^4)^2}{(1-x)^3}$ for 0.2 < x < 0.8, where ν and E are Poisson's ratio and Young's modulus, respectively. F is the force applied to the specimen, B is the specimen thickness, and W is the specimen width (W = 2B). To evaluate the energy release rate at elevated temperatures, the following values of Young's modulus were used: 1200 MPa at 30 °C, 960 MPa at 40 °C, 770 MPa at 50 °C, and 610 MPa at 60 °C. These values were taken from the literature based on the measured value of Young's modulus of the polypropylene at room temperature and on its degree of crystallinity [15]. A value of 0.45 was used for Poisson's ratio ν [16].

Fracture tests were also performed in accordance with ASTM D5045 to measure the critical energy release rate of the polypro-

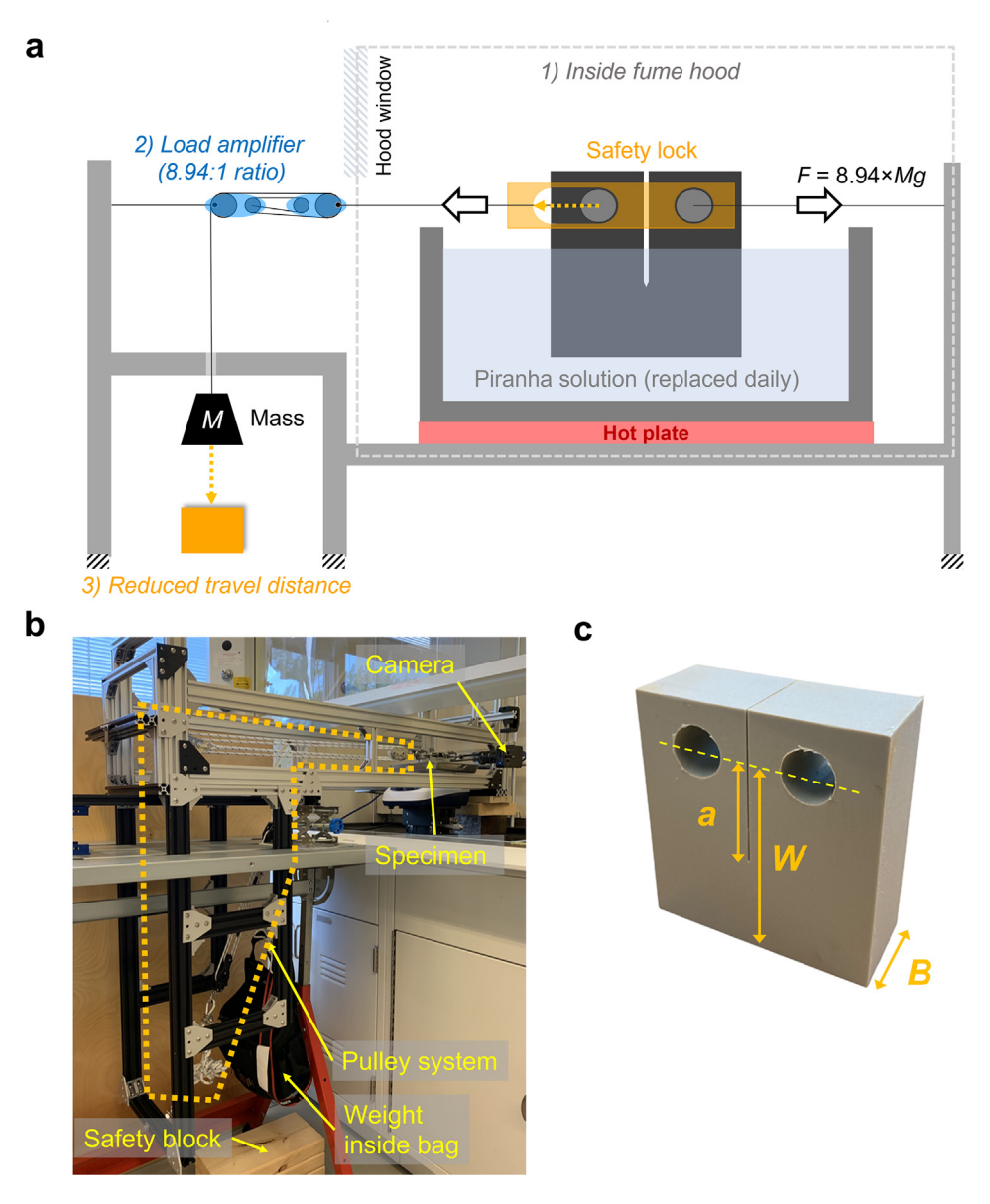


Fig. 2. (a) Schematic diagram and (b) Optical image of custom constant-force loading system with high-temperature oxidizing environment; (c) Optical image of a polypropylene compact tension specimen.

pylene. Compact tension specimens were tested at room temperature and at 50 $^{\circ}$ C with a universal testing machine using a crosshead displacement rate of 10 mm/min, and the critical energy release rate was calculated using Eq. (1).

Additionally, to evaluate the chemical degradation of polypropylene, 2.0 mm thick samples were exposed for one day to a Piranha solution at 50 °C. After degradation, the samples were observed using a scanning electron microscope (SEM) and characterized using Fourier-transform infrared spectroscopy (FT-IR). To characterize the degree of oxidation, the carbonyl index (CI) was calculated from the FT-IR results using [17–19],

$$CI = \frac{\text{Area under band } 1850 - 1650 \text{ cm}^{-1}}{\text{Area under band } 1500 - 1420 \text{ cm}^{-1}}.$$
 (2)

The carbonyl index is the ratio between the carbonyl (-C=O) and the methylene (-CH₂-) absorption bands and is a measure of the amount of carbonyl species formed during exposure to the Piranha solution. Since many oxidation reactions of polypropylene involve the formation of a carbonyl moiety, the degree of oxidation of polypropylene can be evaluated using the carbonyl index [18,20].

3. Result and discussion

Degradation of Polypropylene in Piranha solution

The Piranha solution is a mixture of concentrated sulfuric acid and hydrogen peroxide. When combined, these chemicals form peroxymonosulfuric acid (H₂SO₅, Caro's acid), the active oxygen transfer species in the system [21] and one of the strongest known oxidizing chemicals [22], through the following reaction

$$H_2SO_4 + H_2O_2 \leftrightarrow H_2SO_5 + H_2O.$$
 (3)

To compare the oxidizing effect of peroxymonosulfuric acid with that of the individual components of the mixture, polypropylene specimens were exposed for 24 h to a 100% Piranha solution, to 93% sulfuric acid, or to 30% hydrogen peroxide at a temperature of 50 °C. Fig. 3a shows the value of the carbonyl index after exposure to each solution; Fig. 3b shows a series of SEM micrographs of the surfaces of the samples before and after exposure. It is evident from the carbonyl index that exposure

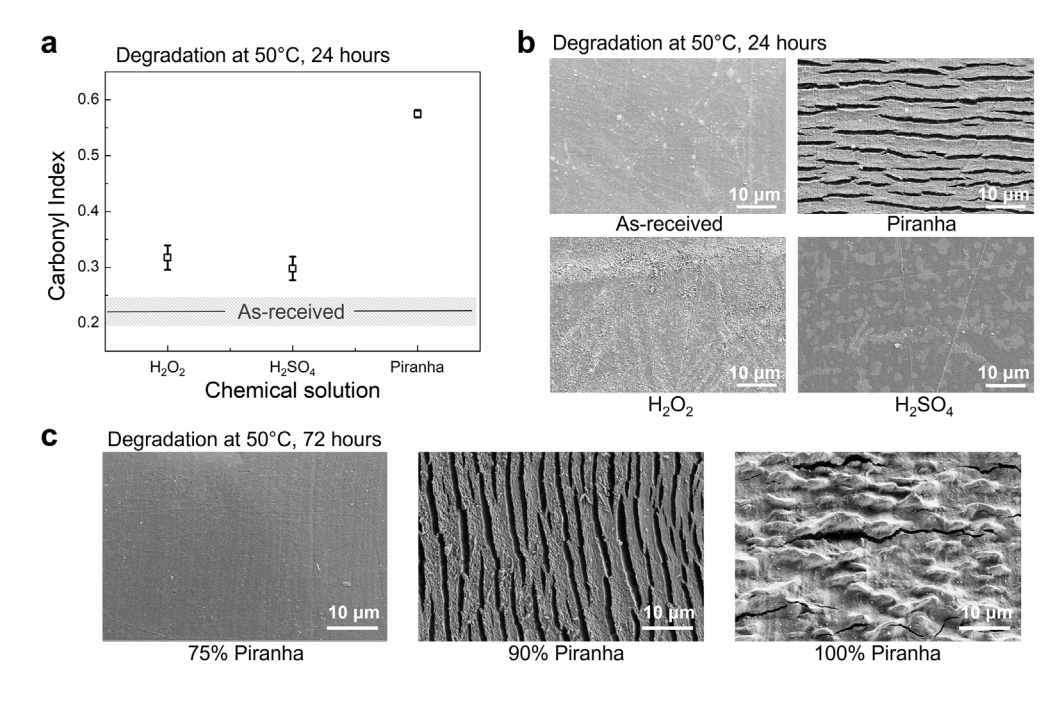


Fig. 3. (a) Carbonyl Index data for polypropylene samples exposed to hydrogen peroxide, sulfuric acid, and 100% Piranha solution at 50 °C for a period of 24 h; (b) SEM images of the polypropylene samples referred to in (a); (c) SEM images of polypropylene samples exposed for a period of 72 h to 50 °C Piranha solutions of different concentrations (75, 90, 100%).

to the Piranha solution results in much more extensive oxidation than exposure to either the sulfuric acid or the hydrogen peroxide alone. This is also reflected by the SEM micrographs: The surface exposed to the Piranha solution shows extensive cracking, while the surfaces exposed to sulfuric acid or hydrogen peroxide are relatively unchanged. To evaluate the effect of the peroxymonosulfuric acid concentration on the oxidation of polypropylene, exposure experiments were also performed on polypropylene specimens in Piranha solutions of various dilutions. Fig. 3c shows the polypropylene surfaces after exposure to three different concentrations (75%, 90%, 100% of the nominal Piranha solution, balance deionized water) at 50 °C for 72 h. The specimen exposed to the 100% Piranha solution shows significant erosion of the surface, with a few surface cracks. Comparing images in Fig. 3b and 3c, it is evident that exposure to the 100% solution first causes a high density of surface cracks. Continued exposure, however, erodes the surface sufficiently to remove all but the deepest surface cracks. These observations, along with the alignment of the surface cracks, suggest that residual stresses in the surface of the sample or possibly microstructural features play a role in this process. Exposure to the 90% solution similarly results in a high density of surface cracks, while exposure to the 75% solution has little effect on the surface of the sample (Fig. 3c). These observations indicate that the rate of degradation of polypropylene is a sensitive function of the concentration of the Piranha solution.

Fracture behavior of polypropylene

One of the characteristics of stress-corrosion cracking is that crack growth occurs at energy release rates *below* the critical energy release rate G_c , because species in the environment react with the material at the crack tip promoting crack growth [9]. Sub-critical crack growth testing is the primary method for characterizing SCC — in this method, crack velocity is measured under sub-critical conditions, i.e., under conditions where the applied energy release rate is lower than G_c , and thus insufficient to cause fast failure of the sample.

Thus, prior to making the subcritical measurements, fracture tests were performed using CT specimens to find the critical energy release rate. The measured value of G_c is 14.4 \pm 1.4 kJ/m² at 19 °C, and 15.6 kJ/m² at 50 °C (Fig. 4a). These measurements agree with a report in the literature that the fracture energy of polypropylene with a crystallinity of 50% increases only slightly with temperature, with little or no change below 80 °C [23]. The color of a pristine polypropylene specimen is grey, but the fracture surface of the samples is whitened after the testing. This whitening occurs because micro-voids form along the crack path as a result of plastic deformation [24,25]. The polypropylene is very ductile as illustrated by the stress-strain curve at the bottom of Fig. 4a: The stress-strain curve goes through a maximum and the tensile specimen develops a neck that propagates at constant stress along the gauge length of the specimen. As the neck propagates, the specimen does not deform further in either the necked or un-necked regions and the imposed displacement is entirely accommodated by the propagation of the neck. The plastic strain associated with neck formation is between 35%-40% and the necked region has a similar whitened appearance as the fracture surfaces. Thus, the whitening observed during critical fracture is indicative of ductile fracture.

Fig. 4b shows fracture specimens that were tested under four different conditions: Specimens were tested either in 50 °C DI water or in a 50 °C Piranha solution, and a constant energy release rate was applied that was either well below G_c (\sim 6% of G_c) or approximately equal to G_c . The case where the sample was tested in DI water and the applied energy release rate was equal to G_c is a critical fracture experiment that resulted in a ductile crack with significant whitening in the region of the crack tip. When the same experiment was performed in the Piranha solution, however, the specimen initially exhibited ductile fracture and then transitioned to brittle fracture as illustrated in Fig. 4c. The precise reason for this transition is not known but may be related to the presence of antioxidant compounds in the specimen, which may initially delay the effect of the Piranha solution. Since ductile fracture in polypropylene is accompanied by extensive plastic

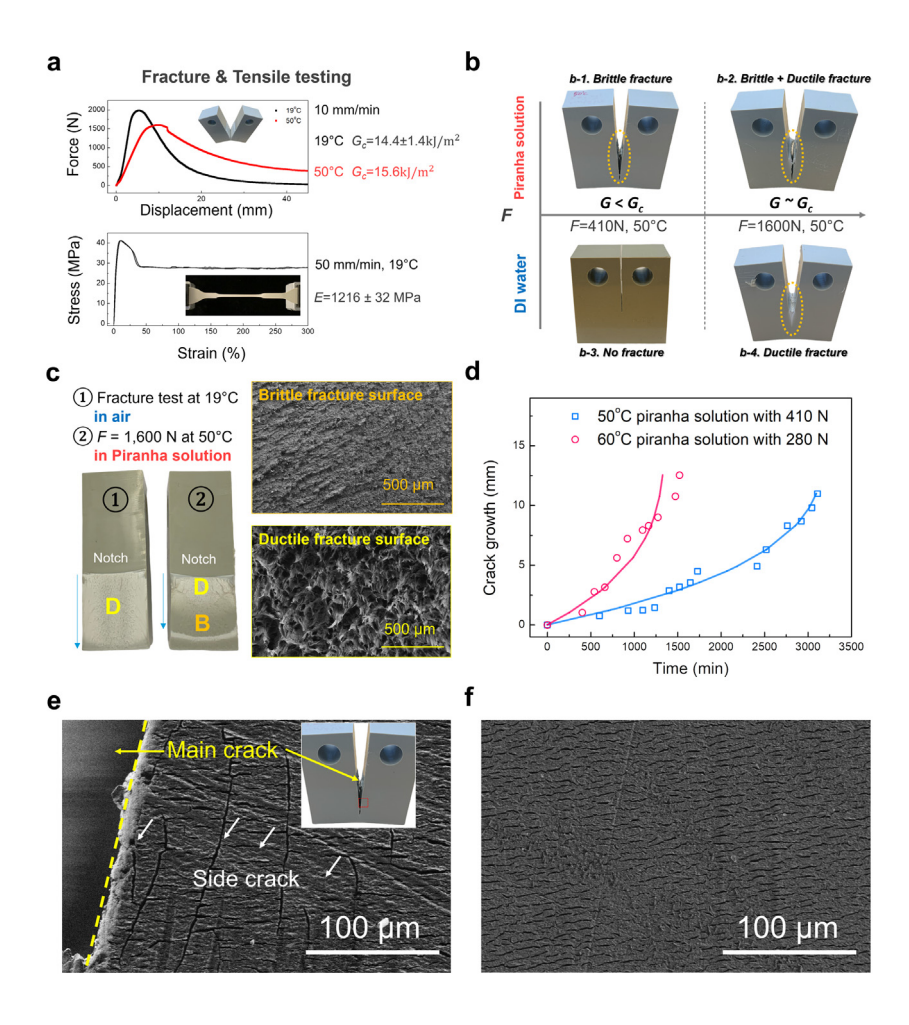


Fig. 4. (a) Compact tension fracture test and uniaxial tensile test results of polypropylene specimens; (b) Specimens after crack growth testing with applied energy release rate under/at G_c with/without Piranha solution at 50 °C; (c) Optical images of a ductile sample (19 °C specimen from Fig. 4a) and a mixed ductile/brittle sample (b^{-2} specimen from Fig. 4b), and SEM images of ductile and brittle fracture surfaces; (d) Graph of crack growth versus time for specimens in a 100% Piranha solution at 50 °C subject to a constant force of 410 N and at 60 °C subject to a constant force of 280 N; (e) SEM image of polypropylene CT specimen near crack path after degradation in a 50 °C Piranha solution with 410 N for 53 h; (f) SEM image of polypropylene after degradation in a 50 °C Piranha solution for 53 h without applied force.

deformation and micro-void formation, the resulting fracture surface is rough and porous. Brittle fracture, on the other hand, does not involve micro-void formation and leads to relatively smooth and flat fracture surfaces (Fig. 4c).

To minimize plastic deformation during fracture, specimens were also tested by applying an energy release rate of approximately 6% of the critical value. Not surprisingly, the specimen tested in deionized (DI) water did not show any crack growth. However, as illustrated in Fig. 4b, the specimen tested in the 50 °C Piranha solution showed significant crack growth over time. During crack propagation, the crack remained sharp with no evidence of plastic deformation or micro-void formation. Fig. 4d shows the evolution of the crack length as a function of time at 50 °C and 60 °C, respectively. At the onset of the experiment, the applied energy release rate is approximately 6% of the critical energy release rate, but as the crack length increases with time, so does the energy release rate, and the rate of growth rises. Note that the number of measurements in Fig. 4d is limited to minimize the risk of exposure to the Piranha solution during the experiments.

Fig. 4e shows a scanning electron microscopy (SEM) image of a CT specimen after testing in the Piranha solution. It is evident that, in addition to the crack that was initiated at the notch in

the CT specimen, a number of cracks developed parallel to the main crack. Fig. 4f shows an SEM image of a CT specimen that was exposed to the Piranha solution for the same amount of time, but without any load applied to the specimen. In this case, a large number of small cracks developed in the surface of the polypropylene that were all more or less aligned in the same direction. Clearly, exposure to the Piranha solution results in the nucleation and growth of cracks in polypropylene. Furthermore, the orientation of the cracks suggests that they grow in directions dictated by the local stress state (Fig. 4e, 4f), or possibly the microstructure of the material (Fig. 4f).

These observations are consistent with observations of the fracture behavior of polypropylene when exposed to other oxidizing agents, such as ozone [26], high-temperature air [27], and UV light [14,28]. The details of the oxidation process are complex and depend on the active species involved, but oxidation generally causes scission of the polypropylene chains, and cracks form in the surface of the polypropylene, possibly as a result of residual stresses in the surface layer of the samples [5,29]. There is evidence that the chain scission process depends on the stress state of the polypropylene, with tension accelerating the scission process, and compression slowing it down [14,30]. The results in Fig. 4d suggest that similar processes also take place at the

crack tip when polypropylene is exposed to the Piranha solution, as a result of reaction with the oxidizing species present in the solution. Oxidation results in scission of the polypropylene chains at the crack tip and the crack propagates with little or no evidence of plastic deformation. As the crack grows with time, the applied energy release rate increases, and the crack velocity rises.

The scatter in the measurements in Fig. 4d suggest that the cracks grow in a somewhat discontinuous fashion with short periods of incubation followed by rapid propagation. Polypropylene nearly always contains antioxidants such as phenolic and phosphite compounds to stabilize its properties and prevent degradation when exposed to oxygen [8]. X-ray photoelectron spectroscopy scans of polypropylene samples before and after exposure to a Piranha solution are shown in Appendix B. The scan obtained prior to exposure contains a number of peaks that disappear after exposure and that are presumably associated with the antioxidants. Initially, these antioxidants prevent scission of polypropylene chains by the oxidizing species in the Piranha solution and the crack does not propagate. However, with time, the antioxidants at the crack tip are sufficiently depleted, chains undergo scission by reacting with the oxidizing species, and the crack propagates in a brittle fashion. As fresh polypropylene is exposed, this process repeats itself an eventually a quasi-steady state develops where the crack propagates at a rate that allows depletion of the antioxidant at the crack tip and ensuing chain scission.

Crack growth curves and the effect of temperature

Fig. 5a shows the crack velocity (da/dt) as a function of applied energy release rate at various ambient temperatures. As expected, the curves increase monotonically with increasing energy release rate and shift to higher values as the temperature increases. Crack velocity curves for materials that are susceptible to stress-corrosion cracking often have several distinct stages as the applied energy release rate increases [6,9,31,32]: there is an initial stage, where the velocity rises exponentially with energy release rate, followed by a stage where the velocity rises much more slowly. The exponential rise is usually associated with the range of energy release rates where crack growth is controlled by the chemical reaction at the crack tip, while the second stage is associated with a regime where crack growth is controlled by transport of the active species to the crack tip. The results in Fig. 5a, however, suggest that in our experiments, there is only one stage with a sublinear dependence of crack velocity on energy release rate. Consequently, we describe the dependence of the crack growth rate on the applied energy release rate using a single power law. For a given applied energy release rate, more elevated temperatures result in higher crack growth rates. If the process that controls crack growth is thermally activated, the crack velocity may be described by an Arrhenius-type equation of the form [10,33].

$$\frac{da}{dt} = A \exp\left[-\frac{\Delta H}{RT}\right] G^n,\tag{4}$$

where ΔH is the activation energy for the rate controlling mechanism, R is the ideal gas constant, A and n are fitting parameters. The exponential factor on the righthand side of this equation describes the temperature-dependence of the mechanism that controls crack growth; the power law factor provides a phenomenological description of the effect of the energy release rate. If, at different values of the energy release rate, the crack velocity becomes limited by a different process, then a different activation energy may need to be used in this regime.

Instead of fitting Eq. (4) to the crack velocity data as is common practice in subcritical fracture experiments, we fit the integrated form of Eq. (4) directly to the crack length as a function of time (Fig. 4d). While more difficult to execute, this approach

obviates the need to take the numerical derivative of experimental data. We believe that this analysis method is beneficial for subcritical experiments where the number of data points is limited because of safety considerations and where there is significant scatter in the data. The value of n was determined to be approximately 0.9 by performing a least-squares fit of all the crack length data in Fig. 4d. The curves in Fig. 4d and in Fig. 5a represent crack length and velocity according to Eq. (4) with an n-value of 0.9.

Fig. 5b is an Arrhenius graph of $\ln(da/dt/G^n)$ for all experimental data in Fig. 5a. The slope of this graph yields a value of 99.7 \pm 15.3 kJ/mol for the activation energy of subcritical crack growth of polypropylene in Piranha solutions. For comparison, previous studies measured the activation energy of several polypropylene degradation processes using thermogravimetric analysis (TGA) [34,35]. The activation energy for thermal degradation in an N₂ or Ar environment was in the 150–250 kJ/mol range, while the activation energy for thermo-oxidative degradation of polypropylene was measured to be 80–110 kJ/mol.

The mechanism that controls the rate of crack growth is not known at this time. While the activation energy for crack growth in the presence of Caro's acid is similar to the activation energy for thermo-oxidative degradation of polypropylene, the dependence of crack velocity on energy release rate is not exponential as expected in the case that the velocity is controlled by stress-assisted chain scission at the crack tip [36,37]. One possible explanation for the latter observation is that some plasticity at the crack tip reduces the effect of stress at more elevated values of the energy release rate. Other mechanisms cannot be ruled out, however, including that transport of the reactive species to the crack tip is the rate limiting step or that crack propagation is limited by the rate of formation of Caro's acid near the crack tip. In fact, the activation energy for the rate of formation of Caro's acid is also approximately 110 kl/mol [38].

Effect of chemical concentration on stress corrosion crack growth

Fig. 6a shows the crack growth rate as a function of the applied energy release rate at a temperature of 50 °C for samples exposed to various dilutions of the Piranha solution. The solid curves in the figure are least-squares fits of the integrated form of Eq. (4) with n of 0.9 to the crack growth data where only the temperaturedependent pre-factor was allowed to vary. As expected from the exposure experiments, the crack velocity at a fixed energy release rate increases rapidly with the concentration of the Piranha solution. This is better illustrated in Fig. 6b, which shows the crack velocity at a fixed energy release rate of 10 kJ/m² as a function of the concentration of Caro's acid. The concentrations were calculated from the initial concentrations of the reagents used to make the Piranha etch and the equilibrium constants measured by Monger and Redlich [38]. It is evident from the figure that the crack velocity decreases almost linearly with decreasing molarity of Caro's acid and that the crack velocity approaches zero when the concentration of Caro's acid drops below approximately 0.6 M. It is also evident that the molarity of Caro's acid decreases rapidly as the Piranha solution is diluted.

Practical guidelines for preventing SCC with G-da/dt curve

Knowledge of the *G-da/dt* relation for polypropylene in various oxidizing environments makes it possible to predict the growth of flaws in polypropylene structures, thus preventing premature failure and improving safety. In particular, we can estimate the remaining service life of a component using a real flaw found through in-service inspection or calculate the expected service life of a component using a postulated flaw during the design. Estimating the remaining service life makes it possible to determine a cost-effective replacement cycle for components considering both safety and production schedule. Calculation of the expected

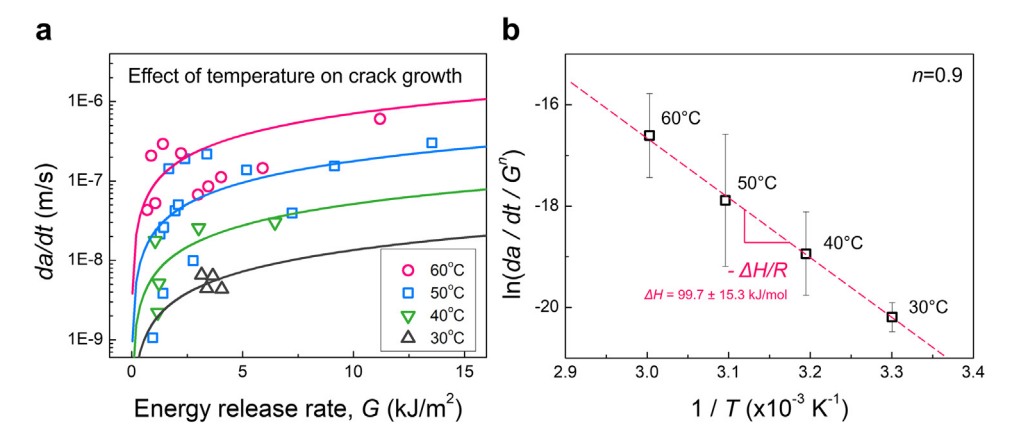


Fig. 5. (a) Crack growth rate as a function of energy release rate at different temperatures: 30, 40, 50, 60 °C; (b) Arrhenius plots for polypropylene: crack growth rate in 100% Piranha solution, determined using all experimental data in Fig. 5a with n = 0.9.

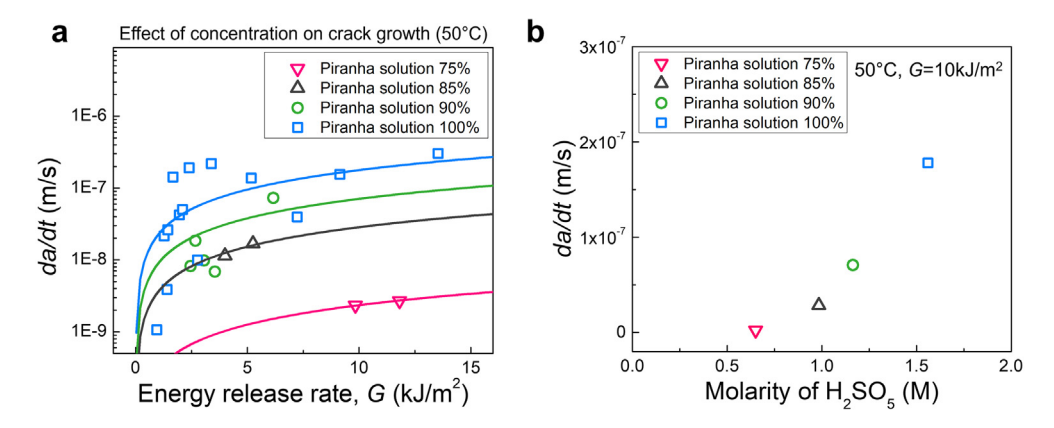


Fig. 6. (a) Crack growth rate as a function of energy release rate at the different concentrations at 50 °C: 75, 85, 90, 100%; (b) Plot of crack growth rate as a function of H_2SO_5 molarity at $G = 10 \text{ kJ/m}^2$.

service life in various environments allows a clear determination of safe operating conditions for a component. The American Society of Mechanical Engineers Boiler & Pressure Vessel Code (ASME BPVC) Section XI [33], which is widely applied to inservice inspection and testing of nuclear power plants, specifies the *K-da/dt* master curve of SCC for several metallic materials and shows how these curves can be used in flaw growth analysis. ASME BPVC Section XI suggests a linear elastic fracture mechanics (LEFM)-based, non-ductile fracture evaluation method to prevent premature failure. Given that polypropylene is prone to brittle fracture in strong oxidizing environments, we use a similar approach to estimate the time to failure for polypropylene component in such environments.

Inspection Guideline. During inspection, flaws are evaluated using a non-destructive method such as Phased Array Ultrasonic Testing (PAUT). Measured flaw sizes are then used to determine the remaining service life of the component by analyzing the crack growth based on the G-da/dt curve. Fig. 7a is a schematic flow chart describing the procedure for assessing the remaining service life of a pipe based on ASME BPVC Section XI Nonmandatory Appendix C. Before the inspection, two pieces of information are needed: (1) the critical energy release rate G_c and (2) the G-da/dt relation for the environment of interest. During the inspection, the inspector evaluates the flaw size (a) using a nondestructive method. Given the flaw size, geometry, and stress state, the energy release rate G can be evaluated for the flaw. If the value of G is larger than G_c , the pipe should be replaced

immediately. If the value is smaller, then the G-da/dt curves obtained in this study can be used to calculate the time required for the flaw to reach critical size. This time is the remaining service life of the pipe. For this calculation, it is necessary to calculate the crack growth for a specific time interval t using the G-da/dt relationship, and then repeat the analysis with the new crack length. Here, a sufficiently small t should be used for precise calculations [33].

Design Guideline. The expected service life of a component in a particular environment can be calculated using the G-da/dt relationship if a postulated flaw size is used instead of an actually measured flaw size (Fig. 7b). In this case, the procedure in Fig. 7a may be used to select operating conditions to satisfy a minimum required service life. Consider the following example. Cracks in a pipe generally propagate in the directions perpendicular to the hoop direction, hence we assume a semi-elliptical flaw perpendicular to the hoop direction in the inner surface of the pipe and take its aspect ratio (a/l) equal to 0.1667 [39], where a is the crack depth and l is crack length. The smallest flaw that can be detected using PAUT is approximately 0.8 mm [40] and this value is taken as the depth of the postulated flaw (a). To calculate the energy release rate for the flaw, the hoop stress, σ , acting on the flaw is required (Fig. 7c). Generally, extruded polypropylene pipes have molding stress levels of less than 5 MPa [28,41], but external loads can easily induce additional stress. Consequently, we assume stress levels as high as 20 MPa when calculating the energy release rate. To account for the scatter in the crack

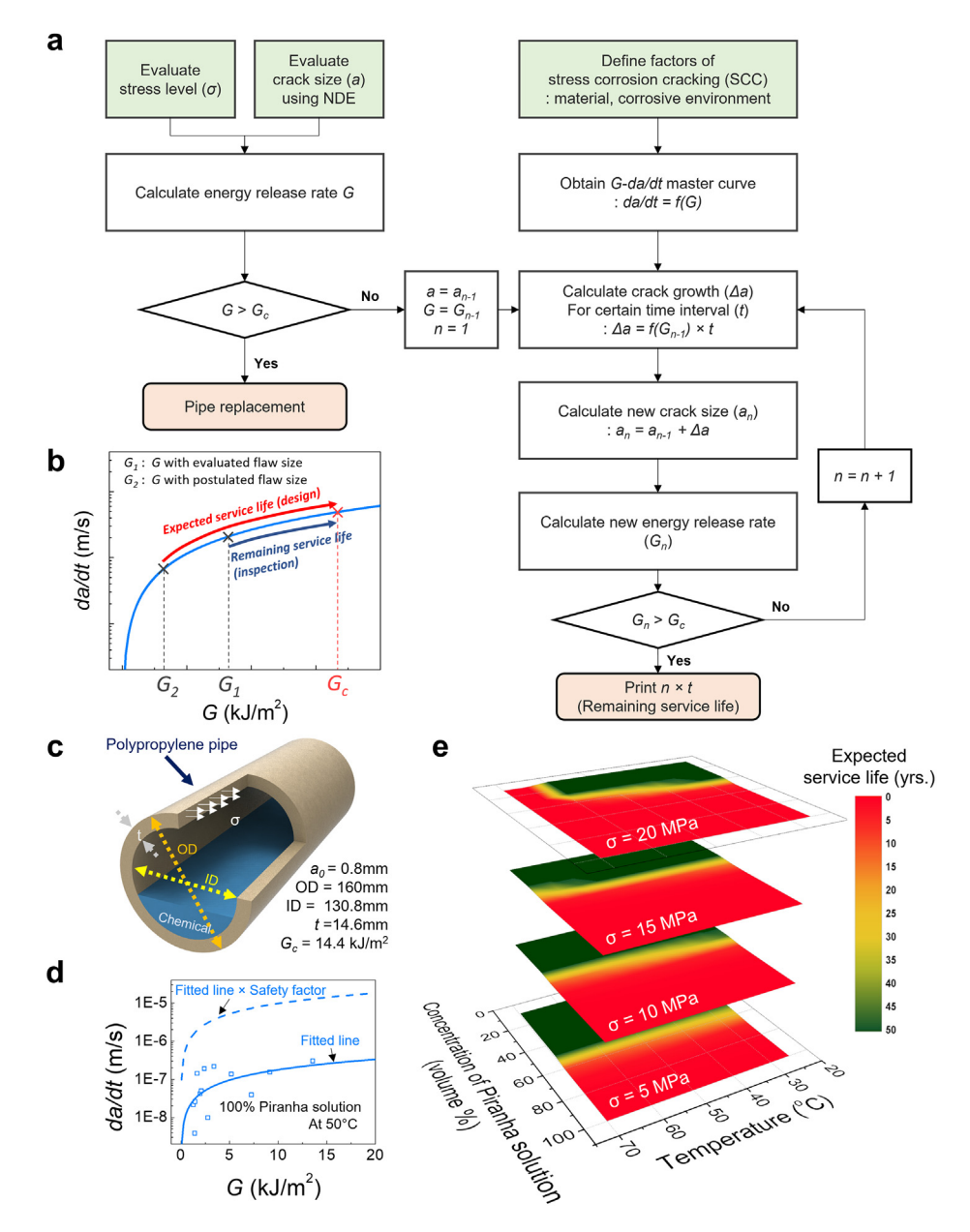


Fig. 7. (a) Flow chart for assessing the remaining service life of a pipe vulnerable to SCC using non-ductile fracture evaluation and G-da/dt curve; (b) Comparison of expected service life and remaining service life on a G-da/dt curve; (c) Schematic diagram of a polypropylene pipe for transporting chemicals; (d) New G-da/dt curve with a safety factor that corresponds to four times the standard deviation of the data around the velocity curve in Fig. 5b; (e) Expected service life of the polypropylene pipe in (c) for transporting Piranha solutions of various concentrations and temperatures at various stress levels. The calculations were performed using a time interval of two weeks and the value of the critical energy release rate G_c at room temperature. (For interpretation of the references to color in this figure legend, the reader is referred to the web version of this article.)

velocity curves, a safety factor that corresponds to four times the standard deviation of the data around the velocity curve was introduced as illustrated in Fig. 7d. This safety factor ensures that our estimate is an upper bound for 99.994% of the velocity data. For each condition, the amount of time was calculated for the flaw to reach critical size. Fig. 7e shows the expected service life for various environments and stress levels. Since many production facilities are built with an expected service life of fifty years, pipe designs with a service life exceeding fifty years are shown in green in Fig. 7d. Evidently, the red area, which represents conditions with an expected service life less than fifty years, expands as the stress level increases. One salient feature of the figure is the strong dependence of service life on the strength of the Piranha solution. In particular, accidental exposure to a

concentrated Piranha solution can significantly reduce the service life of a polypropylene pipe.

4. Conclusion

We have studied stress corrosion cracking of polypropylene in Piranha solutions. We evaluated the rate of subcritical crack growth as a function of the energy release rate over a range of temperatures and concentrations of the Piranha solution. Crack growth rate increases with temperature, and an Arrhenius graph of the rate of growth between 30 °C and 60 °C yields an activation energy of 99.7 \pm 15.3 kJ/mol. Dilution of the Piranha solution with deionized water results in a significant reduction in the crack growth rate. We describe a general inspection guideline

to evaluate the remaining service life of a polypropylene component exposed to the Piranha solution using the *G-da/dt* curve based on the SCC crack growth analysis and non-ductile fracture evaluation specified in ASME BPVC. By introducing a postulated flaw based on available inspection methods, we evaluate the expected service life of polypropylene pipe in Piranha solution under various environments and show that accidental exposure to a concentrated Piranha solution can significantly reduce its service life. We hope that this method will help in the design and safe use of thermoplastic pipes in strong oxidizing environments.

Declaration of competing interest

The authors declare that they have no known competing financial interests or personal relationships that could have appeared to influence the work reported in this paper.

Data availability

Data will be made available on request.

Acknowledgments

This research was supported by Samsung Electronics, South Korea under Grant A47773. The sample characterization was partly performed at Harvard Center for Nanoscale Systems (CNS), which is supported by the NSF, USA under Grant ECS 1541959, and the Harvard University MRSEC, which is funded by the NSF, USA under Grant DMR-2011754.

Appendix A. Differential scanning calorimetry scan of the polypropylene sample

Fig. A.1 shows the differential scanning calorimetry scan of the polypropylene specimen used in this study. The first heating scan shows that the melting temperature of as-received polypropylene is 165.4 °C and the ΔH_m is 104.5 J/g. Using the heat of fusion of 100% crystalline polypropylene (ΔH_m^0), the degree of crystallinity (χ) of the as-received polypropylene specimen was determined to be

$$\chi$$
 (%) = $\frac{\Delta H_m}{\Delta H_m^0} \times 100\% = \frac{104.5 \text{ J/g}}{207 \text{ J/g}} \times 100\% = 50\%$

The crystallization temperature on cooling is of 123.4 °C.

Appendix B. X-ray photoelectron spectroscopy scan of a polypropylene sample before and after exposure to a Piranha solution

See Fig. B.1.

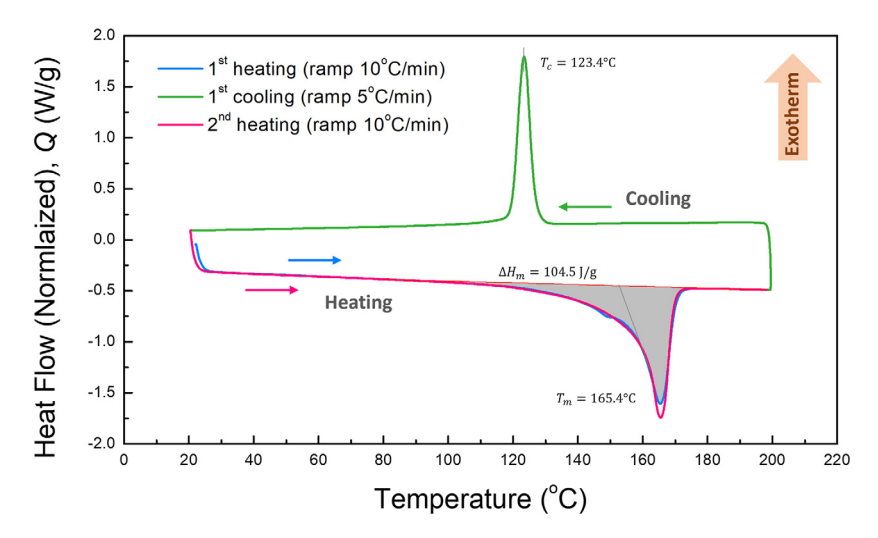


Fig. A.1. DSC measurement of the polypropylene specimen used in this study.

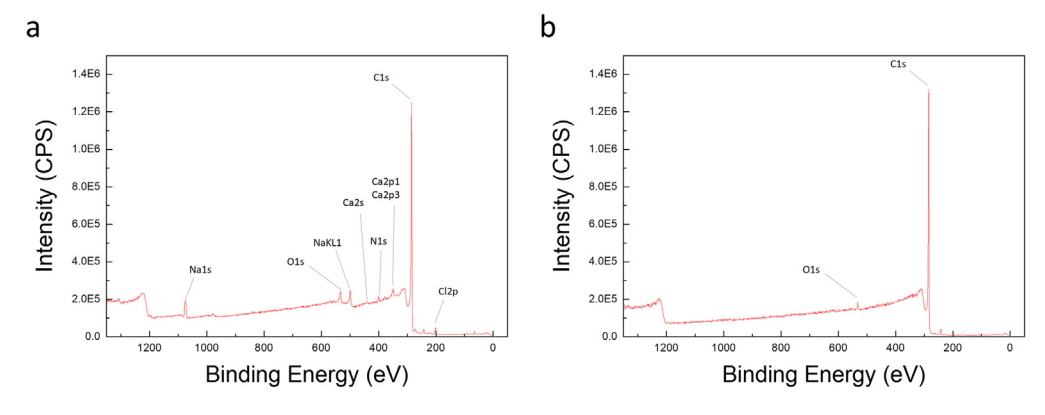


Fig. B.1. XPS results for (a) an as-received polypropylene specimen and (b) a polypropylene specimen after two weeks of degradation in a 55 °C Piranha solution. Before measurements, surfaces of both specimens were etched for 10 min using Ar sputtering.

References

- DIN-DVS 2205-1 Calculation of Tanks and Apparatus Made of Thermoplastics, DIN, 2015.
- [2] D. Court, TR-19/2007 chemical resistance of thermoplastics piping materials, 2007.
- [3] I.T.S. Heikkinen, C. Kauppinen, Z. Liu, S.M. Asikainen, S. Spoljaric, J. v. Seppälä, H. Savin, J.M. Pearce, Chemical compatibility of fused filament fabrication-based 3-D printed components with solutions commonly used in semiconductor wet processing, Addit. Manuf. 23 (2018) 99–107, http://dx.doi.org/10.1016/j.addma.2018.07.015.
- [4] J.B. DeCoste, F.S. Malm, V.T. Wallder, Cracking of stressed polyethylene, Ind. Eng. Chem. 43 (1951) 117–121, http://dx.doi.org/10.1021/ie50493a035.
- [5] B.H. Choi, Z. Zhou, A. Chudnovsky, S.S. Stivala, K. Sehanobish, C.P. Bosnyak, Fracture initiation associated with chemical degradation: Observation and modeling, Int. J. Solids Struct. 42 (2005) 681–695, http://dx.doi.org/10. 1016/j.ijsolstr.2004.06.028.
- [6] A. Chudnovsky, Slow crack growth, its modeling and crack-layer approach: A review, Internat. J. Engrg. Sci. 83 (2014) 6–41, http://dx.doi.org/10.1016/j.ijengsci.2014.05.015.
- [7] B.H. Choi, A. Chudnovsky, K. Sehanobish, Stress corrosion cracking in plastic pipes: Observation and modeling, Int. J. Fract. 145 (2007) 81–88, http://dx.doi.org/10.1007/s10704-007-9092-3.
- [8] B.H. Choi, A. Chudnovsky, R. Paradkar, W. Michie, Z. Zhou, P.M. Cham, Experimental and theoretical investigation of stress corrosion crack (SCC) growth of polyethylene pipes, Polym. Degrad. Stab. 94 (2009) 859–867, http://dx.doi.org/10.1016/j.polymdegradstab.2009.01.016.
- [9] M. Ciccotti, Stress-corrosion mechanisms in silicate glasses, J. Phys. D Appl. Phys. 42 (2009) http://dx.doi.org/10.1088/0022-3727/42/21/214006.
- [10] M.K.V. Chan, J.G. Williams, Slow stable crack growth in high density polyethylenes, Polymer 24 (1983) 234–244, http://dx.doi.org/10.1016/0032-3861(83)90139-8.
- [11] Q. Jiao, M. Shi, T. Yin, Z. Suo, J.J. Vlassak, Composites retard hydrolytic crack growth, Extreme Mech. Lett. 48 (2021) 101433, http://dx.doi.org/10. 1016/j.eml.2021.101433.
- [12] M. Shi, Q. Jiao, T. Yin, J.J. Vlassak, Z. Suo, Hydrolysis embrittles poly(lactic acid), MRS Bull. 48 (2022) 1–11, http://dx.doi.org/10.1557/s43577-022-00368-5.
- [13] H.G. Schmidt, Safe piranhas: A review of methods and protocols, ACS Chem. Health Saf. 29 (2022) 54–61, http://dx.doi.org/10.1021/acs.chas. 1c00094.
- [14] T. Li, J.R. White, Photo-oxidation of thermoplastics in bending and in uniaxial compression, Polym. Degrad. Stab. 53 (1996) 381–396, http://dx. doi.org/10.1016/0141-3910(96)00095-x.
- [15] J. Li, Z. Zhu, T. Li, X. Peng, S. Jiang, L.S. Turng, Quantification of the Young's modulus for polypropylene: Influence of initial crystallinity and service temperature, J. Appl. Polym. Sci. 137 (2020) 1–7, http://dx.doi.org/10.1002/ app.48581.
- [16] P.P. Institute, J. Babcanec, J. Beaver, J. Goddard, C. Jones, L. McCarthy, M. Pluimer, T. Toliver, K. White, J. Ahrenholz, 21st Century Drainage Solutions: PPI Drainage Handbook, CLVR Agency, 2021.
- [17] J. Almond, P. Sugumaar, M.N. Wenzel, G. Hill, C. Wallis, Determination of the carbonyl index of polyethylene and polypropylene using specified area under band methodology with ATR-FTIR spectroscopy, E-Polymers 20 (2020) 369–381, http://dx.doi.org/10.1515/epoly-2020-0041.
- [18] W.S. Subowo, M. Barmawi, O.B. Liang, Growth of carbonyl index in the degradation of polypropylene by UV irradiation, J. Polym. Sci. A 24 (1986) 1351–1362, http://dx.doi.org/10.1002/pola.1986.080240618.
- [19] M.C. Celina, E. Linde, E. Martinez, Carbonyl identification and quantification uncertainties for oxidative polymer degradation, Polym. Degrad. Stab. 188 (2021) 109550, http://dx.doi.org/10.1016/j.polymdegradstab.2021.109550.
- [20] C. Maier, T. Calafut, Polypropylene, William Andrew Publishing, Norwich, NY, 1998, http://dx.doi.org/10.1016/B978-188420758-7.50006-0.
- [21] C.W. Jones, Activation of hydrogen peroxide using inorganic and organic species, in: C.W. Jones, J.H. Clark, C.W. Jones, J.H. Clark, M.J. Braithwaite (Eds.), Applications of Hydrogen Peroxide and Derivatives, The Royal Society of Chemistry, 1999, pp. 37–78, http://dx.doi.org/10.1039/ 9781847550132-00037.

- [22] M. Spiro, The standard potential of the peroxosulphate/sulphate couple, Electrochim. Acta. 24 (1979) 313–314.
- [23] A. van der Wal, J.J. Mulder, R.J. Gaymans, Fracture of polypropylene: The effect of crystallinity, Polymer 39 (1998) 5477–5481, http://dx.doi.org/10. 1016/S0032-3861(97)10279-8.
- [24] A. Pawlak, A. Galeski, A. Rozanski, Cavitation during deformation of semicrystalline polymers, Prog. Polym. Sci. 39 (2014) 921–958, http://dx. doi.org/10.1016/j.progpolymsci.2013.10.007.
- [25] A. Salazar, P.M. Frontini, J. Rodríguez, Determination of fracture toughness of propylene polymers at different operating temperatures, Eng. Fract. Mech. 126 (2014) 87–107, http://dx.doi.org/10.1016/j.engfracmech.2014. 04.023.
- [26] A.A. Popov, N.N. Blinov, B.E. Krisyuk, S.G. Karpova, L.G. Privalova, G.E. Zaikov, Oxidative destruction of polyolefins under stress. The action of ozone on polyethylene and polypropylene, J. Polymer Sci. Polymer Phys. Ed. 21 (1983) 1017–1027, http://dx.doi.org/10.1002/pol.1983.180210703.
- [27] B. Fayolle, L. Audouin, J. Verdu, Oxidation induced embrittlement in polypropylene - a tensile testing study, Polym. Degrad. Stab. 70 (2000) 333–340, http://dx.doi.org/10.1016/S0141-3910(00)00108-7.
- [28] B.O. Donneh, J.R. White, Stress-accelerated photo-oxidation of polypropylene and glass-fibre-reinforced polypropylene, Polym. Degrad. Stab. 44 (1994) 211–222, http://dx.doi.org/10.1016/0141-3910(94)90166-X.
- [29] C. Rouillon, P.O. Bussiere, E. Desnoux, S. Collin, C. Vial, S. Therias, J.L. Gardette, Is carbonyl index a quantitative probe to monitor polypropylene photodegradation? Polym. Degrad. Stab. 128 (2016) 200–208, http://dx.doi.org/10.1016/j.polymdegradstab.2015.12.011.
- [30] A.V. Shyichuk, D.Y. Stavychna, J.R. White, Effect of tensile stress on chain scission and crosslinking during photo-oxidation of polypropylene, Polym. Degrad. Stab. 72 (2001) 279–285, http://dx.doi.org/10.1016/S0141-3910(01)00015-5.
- [31] S.M. Wiederhorn, L.H. Bolz, Stress corrosion and static fatigue of glass, J. Am. Ceram. Soc. 53 (1970) 543–548, http://dx.doi.org/10.1111/j.1151-2916.1970.tb15962.x.
- [32] J.J. Vlassak, Y. Lin, T.Y. Tsui, Fracture of organosilicate glass thin films: Environmental effects, Mater. Sci. Eng. A. 391 (2005) 159–174, http://dx.doi.org/10.1016/j.msea.2004.08.070.
- [33] ASME Boiler and Pressure Vessel Code, Section XI, Division 1, ASME, New York, 2015.
- [34] E. Esmizadeh, C. Tzoganakis, T.H. Mekonnen, Degradation behavior of polypropylene during reprocessing and its biocomposites: Thermal and oxidative degradation kinetics, Polymers 12 (2020) http://dx.doi.org/10. 3390/POLYM12081627.
- [35] J.D. Peterson, S. Vyazovkin, C.A. Wight, Kinetics of the thermal and thermooxidative degradation of polystyrene, polyethylene and poly(propylene), Macromol. Chem. Phys. 202 (2001) 775–784, http://dx.doi.org/10.1002/ 1521-3935(20010301)202:6<775::AID-MACP775>3.0.CO;2-G.
- [36] B.R. Lawn, An atomistic model of kinetic crack growth in brittle solids, J. Mater. Sci. 10 (1975) 469-480, http://dx.doi.org/10.1007/BF00543692.
- [37] R.F. Cook, E.G. Liniger, Kinetics of indentation cracking in glass, J. Am. Ceram. Soc. 76 (1993) 1096–1105, http://dx.doi.org/10.1111/j.1151-2916. 1993.tb03726.x.
- [38] J.M. Monger, O. Redlich, Peroxysulfuric acid and peroxyformic acid. equilibrium and formation rate, J. Phys. Chem. 60 (1956) 797–799, http://dx.doi.org/10.1021/j150540a024.
- [39] J. Lee, J.S. Kim, B. Lee, S. Cho, D. Kwon, J. h. Kim, Effect of post-weld heat treatment conditions on mechanical properties, microstructures and nonductile fracture behavior of SA508 Gr.1a thick weldments, Met. Mater. Int. 27 (2021) 4700–4709, http://dx.doi.org/10.1007/s12540-021-01090-8.
- [40] H. Taheri, A.A. Hassen, Nondestructive ultrasonic inspection of composite materials: A comparative advantage of phased array ultrasonic, Appl. Sci. 9 (2019) http://dx.doi.org/10.3390/app9081628.
- [41] J. Poduška, J. Kučera, P. Hutař, M. Ševčík, J. Křivánek, J. Sadílek, L. Náhlík, Residual stress distribution in extruded polypropylene pipes, Polym. Test. 40 (2014) 88–98, http://dx.doi.org/10.1016/j.polymertesting.2014.08.006.